

How to recover strong ground motion from the behavior of simple structures: the case of Azores earthquake 1998

Carlos Sousa Oliveira

Instituto Superior Técnico/Ceris/Universidade de Lisboa

Abstract: When we lack substantial information from strong motion stations, we may attempt to identify a few simple structures whose behavior can indicate the strength of ground motion. We employ similar procedures to assign macroseismic intensity values to a location by assessing the effects of ground motion on objects, people, and the environment. Our approach involves examining the behavior of simple objects like chimneys, statues, movement of objects from their initial position, water waves in containers, etc., to infer the ground motion that may have caused those effects, both qualitatively and quantitatively. We have successfully applied this method in the recent past. In this paper, we focus on the $M_d 6.2$ 1998 Faial, Azores Earthquake, which was recorded at a few stations, and we were able to gather more information about a set of simple structures. With these two sources of information, we were able to enhance our understanding of the wave field in a volcanic environment. Finally, we check from the recorded as well as from the recovered data the wave attenuation for this earthquake.

Keywords: recover strong motion; Azores; July 9 1998 earthquake; indirect measures of shaking

1. Introduction

Earthquakes in the Azores are a critical factor to consider in risk analyses [Borges et al. 2007]. The region is a prime example of multi-hazard analysis, where earthquakes, volcanic eruptions, and landslides occur frequently [Fructuoso 1873]. Situated at the junction of three tectonic plates (Figure 1), the Azores experience very active seismicity [Caldeira et al. 2017]. Initial seismic hazard studies for the Azores were conducted by Oliveira et al. 1990, with subsequent studies on site effects by [Sincraian et al. (1999)]. More recent catalogues by [Nunes et al. 2004; Fontiela et al. 2018] and pioneering studies using fault rupture concepts by [Zonno 1999] have contributed to the development to the new code of actions (2019), the National Code for Seismic Actions (EN-1998-1 and National Annex), which is set to replace the previous National Code (RSA 1983) by the end of 2022.

The first seismic record in the Azores dates back to the $M 5.2$ earthquake on the Terceira/São Jorge Islands in 1973, captured on an analogue device at the Observatório Príncipe de Mónaco in Horta, Faial Island, followed by the 1980 $M 7.2$ Terceira earthquake record. Since 1995, several digital strong motion stations have been installed on Terceira and São Miguel Islands, capturing numerous moderate events. The Faial $M_d \approx 6.0$ earthquake on July 9, 1998, at 05:19 UTC, was recorded on the same instrument as the 1973 and 1980

earthquakes, providing the only near-field record (approximately 15 km from the epicenter). The existing digital strong motion network recorded this event at five stations on Terceira and São Miguel Islands, with epicentral distances ranging from 50 to 130 km. All seismological stations were saturated except for the downhole components of the IRIS (Chã de Macela) station in São Miguel (Dessai et al., 1999). The accelerometric network maintained by IST, was the only one in the Azores Archipelago. Between 1995 and 2015, the network was expanded with modern stations on Faial, Pico, São Jorge, Graciosa, Terceira, and São Miguel Islands. While these stations captured some records, no significant events occurred during this period. From 2015 onwards, a protocol between IST/Instituto Superior Técnico and IPMA/Instituto Português do Mar e da Atmosfera transferred all management, data acquisition, and processing responsibilities from IST to IPMA, integrating it into the Portuguese Seismographic Stations Network (Carrilho et al. 2021). The present work provides a brief overview of the records collected during this period, focusing exclusively on the 1998 records and their key characteristics. Additionally, by interpreting the structural behavior of various simple structures damaged by the earthquake, we discuss the type of motion acting at their foundations, offering insights into the seismic wave field generated by the event and its aftershocks.

Since the SM network comprised only a limited number of stations, it is crucial to estimate the approximate motion in

terms of PGA (Peak Ground Acceleration) or PGD (Peak Ground Displacement) at other locations to enhance our understanding of the wave field. We have previously achieved this with quite interesting results, and we applied the same technique to develop GMPE's for the Azores Archipelago for the 1998 earthquake data.

The Strong Motion Network in the Azores expanded from one SMA-1 analogue transducer in 1973 to 17 digital stations with 16-21 bit resolution by 2015, recording approximately 450 3-component records belonging to 250 events (Ambraseys et al., 2000; Vilanova et al. 2009; Oliveira, 2025).

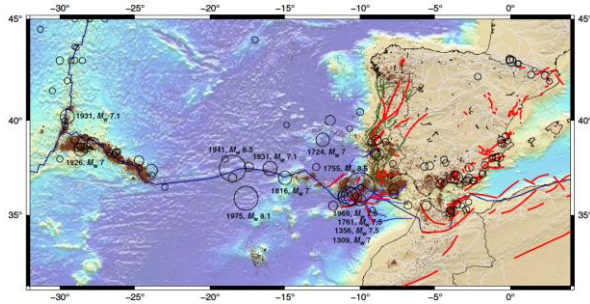


Figure 1. Seismicity of the Azores–Madeira–Iberia region and the contact of three plates (Euro-Asiatic; Nubia and American). Earthquakes recorded instrumentally since 1961 are shown by small brown dots. Historical earthquakes from the Seismic. Harmonization in Europe (SHARE) European Earthquake Catalog (SHEEC), with magnitudes larger than 5.5, are shown by circles whose radiuses correlate to the magnitude of the earthquakes (Stucchi et al., 2013). The earthquakes with magnitudes equal to or larger than 7.0 are labeled with year of occurrence and magnitude. The Archipelago of Azores is highlighted in pale yellow.

2. The 1998 Faial Earthquake

The $M_d \approx 6.0$ earthquake on July 9, 1998, at 05:19 UTC, as already referred was recorded by an analogue strong motion SMA-1 instrument at the Observatório Príncipe de Mónaco in Horta, Faial. This remains up to date the only record obtained in the near-field, approximately 15 km from the epicenter¹. The existing digital strong motion network captured the event at five stations on Terceira and São Miguel Islands, with epicentral distances ranging from 50 to 130 km (Figure 2).

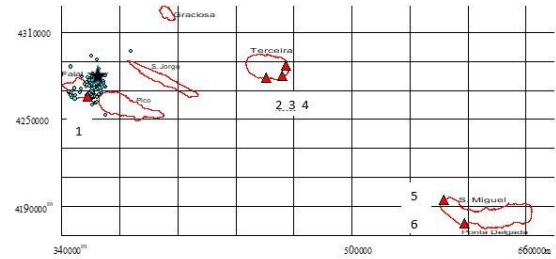


Figure 2. The accelerographic network in the Azores at the date of the earthquake of 9 June 1998. Epicenters of the main events associated with the crisis; Δ stations; \bullet epicenters; \star Main earthquake epicenter. (1- Príncipe de Mónaco Observatory; 2- GZCAH; 3- São Sebastião; 4- Praia da Vitória; 5- Mosteiros; 6- LREC).

Following the main event, numerous aftershocks occurred (Senos et al., 2008), with some being recorded at various digital stations within the strong motion network. By analysing the structural behaviour of several simple structures damaged by the earthquake, we explore the type of motion impacting their foundations, providing insights into the seismic wave field generated by the event and its aftershocks. Figure 3 offers a detailed account of the possible mechanism of the 5:19 event, based on the predominant direction of the aftershocks (Dias and Matias, 2008). As there was no evidence of a fault trace to originate this event two main solutions were discussed by several researchers (Borges et al. 2007).

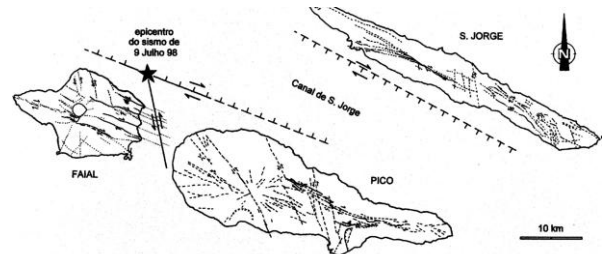


Figure 3. Location of the main faults in the Azores Archipelago and rupture mechanism for the July 9, 1998 earthquake, as proposed by Madeira et al. /8/.

2.1 Analogue record

The main recorded motion occurred at the Observatório Sismológico in Horta, Faial Station (Oliveira, 2008). This event was characterized by very strong shaking with a long duration, as anticipated from the extensive fault rupture that caused it. The three components are illustrated in Figure 4 which only show the first 9 seconds. The main characteristics of the records are presented in Table 2, following processing with the Seismosoft software (2021).

The record exhibits high-frequency content, as shown in the Fourier and Response Spectra in Figures 5 and 6, respectively.

¹ The analogue record obtained during the 1980 Terceira earthquake was at a distance from rupturing fault of approximately 85 km.

The predominant period is 0.04 seconds for both horizontal components and 0.08 seconds for the vertical component. Most energy is concentrated up to 0.2 seconds ($> 5\text{Hz}$). However, a plateau between 0.2 and 0.8 seconds with large spectral values is still present. Amplitudes of horizontal components exceeding 0.5 g persist for more than 20 seconds in a stationary manner, with a significant duration lasting for 32 seconds.

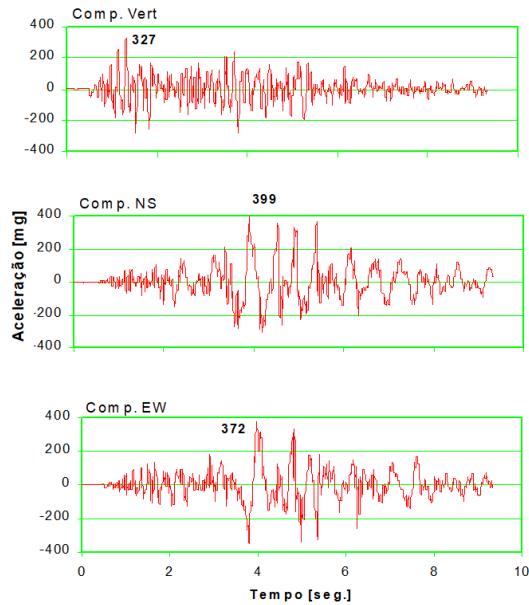


Figure 4 Time-histories of the vertical, N-S and E-W components of the 5:19 event as recorded in the SMA-1 instrument

Figure 4 a), b), c) presents the vertical, N-S and E-W components, having a large velocity pulses. E-W component has a trend similar to N-S one. To produce these traces, a prior signal treatment was applied to the original raw data: linear baseline correction and a 4-pole Butterworth band-pass filter (0.2-20 Hz). (Seismosoft, 2021). Peak values and duration are presented in Table 1

Table 1. Peak values of each component after applying the filtering technique.

| Component | NS | EW | Vert |
|---------------------------------|-------|-------|-------|
| Max Acceleration (mg) | 399 | 372 | 327 |
| Max Velocity (cm/s) | 30 | 37 | 8 |
| Max Displacement (cm) | 3.9 | 2.8 | 0.8 |
| Significant Duration (seconds)* | 32.20 | 32.90 | 29.50 |

*Guessed from other stations away

The joint analysis of Figures 4 and 5 shows that the horizontal movement is essentially characterized by 4 cycles of great amplitude with frequencies of 2.5 Hz and 2.3 Hz, clearly visible in the E-W and N-S components, respectively. Table 2 present these frequencies. The vertical component, also of great amplitude, presents oscillations with higher dominant

frequencies during the first 9 seconds of the recording (6.2 and 6.7 Hz).

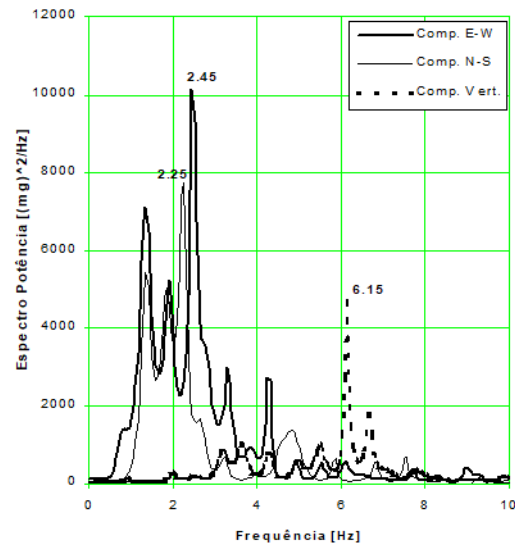


Figure 5. Fourier Spectrum of the 3 components, depicting the predominant frequencies of ground motion.

Table 2. Predominant frequencies [Hz] observed in Figure 6.

| Predominant frequencies [Hz] | | |
|------------------------------|-----|----------|
| E-W | N-S | Vertical |
| 1.4 | 1.4 | 6.2 |
| 1.9 | 1.9 | 6.7 |
| 2.5 | 2.3 | -- |

The response spectra ($\zeta = 5\%$) of the intense phase of the accelerogram are represented in Figure 6, being confronted with the code spectrum (RSA, 1983) for zone A (which includes the city of Horta), type earthquake 1 (near-field) for a type I terrain (rocks and hard coherent soils).

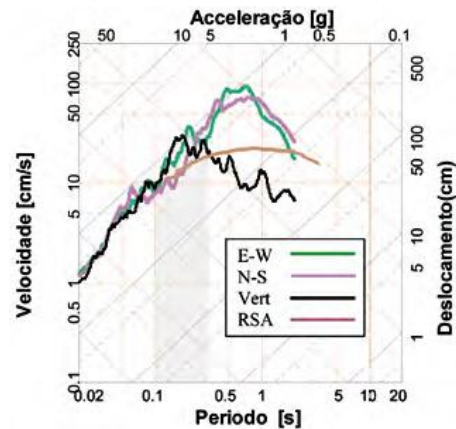


Figure 6. Response spectra for the main event; comparison with the Code spectrum (RSA, 1983) for zone A, earthquake type 1 and terrain type I; 5% damping. (Shaded represents the region where the predominant frequencies of the housing stock of Faial and Pico are located).

From the analysis of Figure 6 it is clear that for periods longer than 0.2 sec, the Code response spectrum presents ordinates systematically lower than those of the main earthquake. Furthermore, it should be noted that the maximum acceleration now recorded is about 2.3 times higher than the value underlying the RSA-1983 (170 cm/s^2).

Analysis of polarization

Figure 7 shows the trace of the particle motion in the horizontal plane showing a predominant component in the NW-SE direction.

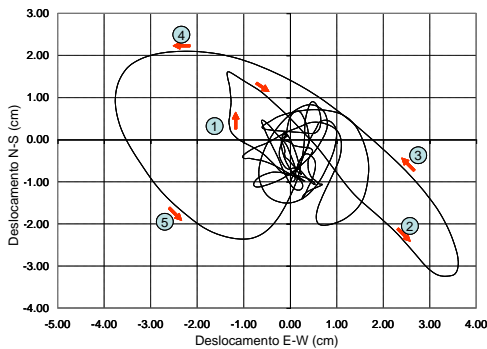


Figure 7. Orbit of movement recorded in the horizontal plane in terms of displacement.

Analysis of the record from the Observatory indicates that the first arrivals, or P waves, are polarized in the NNW-SSE direction and have a predominant frequency of 5 Hz. These are followed by S waves with frequencies ranging from 1.4 to 1.7 Hz, also polarized in the same direction. This direction closely aligns with the believed rupture direction of the fault plane (Senos et al., 2008; Dias et al., 2008; Zonno et al., 2008), as shown in Figure 8. After the initial 4 seconds, the vibration shows a strong movement and low frequency towards the West (largest orbit). Meanwhile, the vertical component exhibits a predominant frequency of 5 Hz, maintaining a nearly constant amplitude during the first 5 seconds of the recording. This component likely had greater amplitude in areas closer to the epicenter, contributing to the loss of friction between the imbricated stones of traditional stone constructions, thereby compromising the structural integrity of this building method.

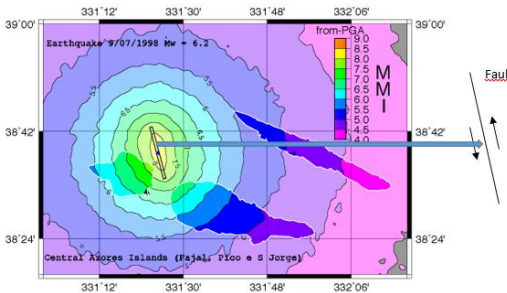


Figure 8. Possible location of the main earthquake rupture according to several authors and simulation of IMM intensities (Zonno et al., 2008).

2.2. Records in digital stations

This section analyzes briefly the records of digital stations, obtained in locations much further away from the epicenter (Figure 2). Some of them (Figure 9) have total durations of more than 75 sec, with, in general, the longest stretches lasting around 15 to 20 sec. The absolute maximum values of the acceleration of the three components of the various records are shown in Table 3.

Table 3. Peak ground acceleration values [mg] of the 5:19 am earthquake recorded in digital stations.

| Stations / Compon. | E-W | N-S | Vertical |
|----------------------|------|------|----------|
| Angra – Ground floor | 15.0 | 19.0 | 12.0 |
| Angra – 3rd floor | 56.0 | 41.0 | 12.0 |
| São Sebastião | 16.6 | 22.6 | 9.7 |
| P. Vitória | 8.7 | 8.9 | 5.4 |
| Mosteiros | 4.5 | 4.1 | 3.2 |

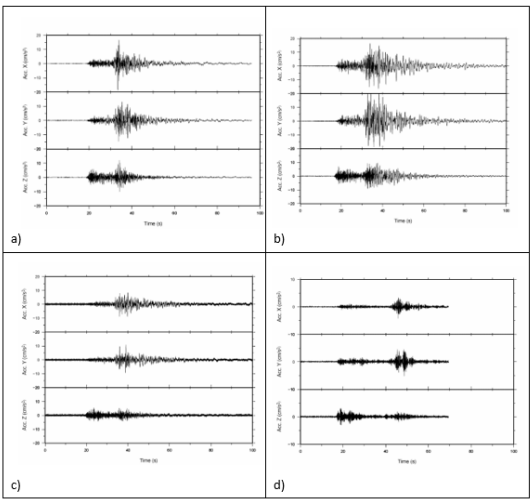


Figure 9. Digital records in the accelerometric network: a) at GZCAH (Angra - Ground Floor); b) in São Sebastião (Terceira); c) in Praia da Vitória (Terceira); d) in Mosteiros (São Miguel).

Figure 10 presents the response spectra of the records obtained in the accelerometric network, with the spectral peaks summarized in Table 4.

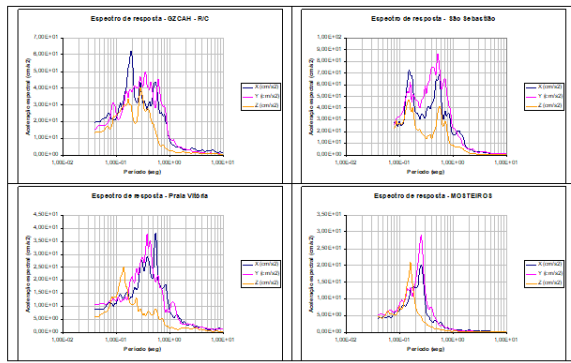


Figure 10. Response Spectra ($\zeta=5\%$) of the digital records in the accelerometric network: a) at GZCAH (Angra - Ground Floor); b) in São Sebastião (Terceira); c) in Praia da Vitória (Terceira); d) in Mosteiros (São Miguel).

Table 4. Values of the dominant frequencies identified in the spectral analysis of the digital network records (Hz).

| E-W | N-S | Vertical |
|-------------------------|-----|----------|
| GZCAH | | |
| 1.6 | 1.4 | 3 |
| 4.4 | 1.8 | 3.2 |
| - | 2.2 | 8.3 |
| São Sebastião | | |
| 1.5 | 1.5 | 1.5 |
| 1.9 | 1.9 | 1.9 |
| 2.4 | 2.5 | 5.7 |
| Praia da Vitória | | |
| 2 | 1.6 | 2 |
| - | 2 | 8.4 |
| - | 2.8 | |
| Mosteiros | | |
| 4.4 | 4.1 | 6.4 |
| - | 4.4 | - |

Table 4 presents the dominant frequencies identified in the power spectra of the digital network records. These generally exhibit low dominant frequencies ranging between 1.0 and 3.0 Hz, even for the vertical components of the movement. Exceptions include the spectra from Mosteiros (São Miguel) and the station installed on the 2nd floor of a building in Angra do Heroísmo, which show higher frequencies. The low frequencies observed are similar to those in the spectra of the horizontal components of the analog station in Horta (Table 2), though this is not the case for the vertical component.

Regarding the polarization of the waves recorded in the digital network in Terceira and São Miguel, it can be summarized as follows: the three records from Terceira are very similar in terms of the orbits in the horizontal plane, showing a polarization of P waves in the NW-SE direction with high frequency and S waves in the N-S direction with lower frequencies.

2.3. Aftershock records

By November 1998, more than 200 aftershocks were recorded on a digital accelerograph placed at the Príncipe de Mónaco Observatory on July 10th Senos (2008).

The largest aftershock, with a magnitude of approximately 4 ($M_d \sim 4$), occurred on July 11th at 00:49 UTC. In addition to being recorded on the digital accelerograph at the Observatory, it was also captured at the Hotel Fayal station (Horta) and at the two stations in the GZCAH building in Angra do Heroísmo. Table 5 presents the maximum acceleration values of the three components from the various records.

Table 5. Absolute peak acceleration values [mg] of the record from the aftershock on July 11, 1998, at 00:49 UTC

| Stations / Comp. | E-W | N-S | Vertical |
|---------------------|------|------|----------|
| Obs. P. Mónaco | 92.0 | 82.0 | 58.0 |
| Hotel Fayal (Horta) | 76.0 | 77.0 | 52.1 |
| Angra – 1st floor | 1.7 | 1.3 | 1.0 |
| Angra – 2nd floor | 8.0 | 8.0 | 1.8 |

It is noteworthy that the record from the Observatory shows large amplitudes and 5 cycles in the N-S component with a frequency of 1.9 Hz.

Figure 11 compares the response spectra of the aftershock on July 11, 1998, at 00:49 UTC with those of the main earthquake.

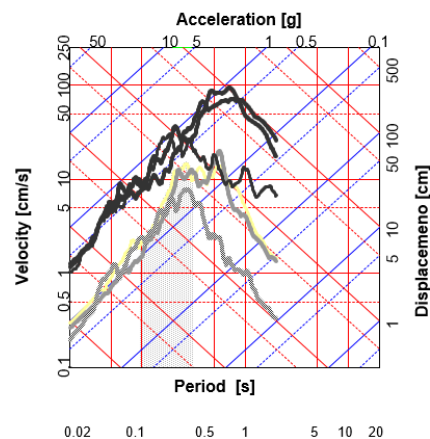


Figure 11. Response Spectra of main shock (black) of July 9 and aftershock (gray) of July 11, 00h49m ($\zeta = 5\%$).

It is evident that the largest spectral ordinates are now found in the range of 0.2 to 0.8 seconds, indicating a concentration of energy at higher frequencies compared to the main shock. This behavior confirms the significant influence of magnitude on the spectral shape. The polarization of the P-waves for this aftershock is NE-SW.

3. Observations related to “site effects”

The analysis of the main earthquake records allows for some additional considerations, particularly regarding "site effects" caused by local geology or topography:

(i) The peak acceleration values recorded at the São Sebastião station are about double (see Table 3) those obtained at the Praia da Vitória station, even though these two stations are nearly the same distance (125 km) from the epicenter. São Sebastião is located within a crater filled with very soft slope deposits (Lopes, 2004). The peak acceleration values of the horizontal components at the São Sebastião station are also slightly higher than those recorded on the ground floor of the building in Angra do Heroísmo, despite this latter station being approximately 11 km closer to the epicenter.

(ii) The ratios of peak accelerations between the base (Hotel Fayal) and the top of the hill at the Observatório Príncipe de Mónaco are generally less than one for all three components of the records. Table 6 presents these ratios for the aftershock on July 11 at 00:49 and for a set of 14 aftershocks during the first three days following the main earthquake.

These observations highlight the significant influence of local geological conditions and topography on seismic response, emphasizing the need to consider site-specific factors in seismic hazard assessments and building design.

Table 6. The ratios of peak accelerations recorded at the base (Hotel Fayal) and at the top of the hill of the Observatório Príncipe de Mónaco in Faial are generally less than one for all three components of the records.

| Events / Components | E-W | N-S | Vertical |
|----------------------------------|------|------|----------|
| Aftershock of July 11, at 00h49m | 0.83 | 0.94 | 0.90 |
| Average of 14 aftershocks | 0.58 | 0.96 | 0.62 |

(iii) The high values of dominant frequencies observed in the records from the second floor of the old building in Angra do Heroísmo reflect the amplification of motion around the building's fundamental period. Table 7 presents the amplification of maximum acceleration between the ground floor and the second floor for both the main earthquake and its primary aftershock. This amplification highlights how the building's structural characteristics can influence its seismic response, especially at its natural frequency, potentially leading to increased motion on higher floors. Understanding these effects is crucial for assessing building safety and designing structures that can better withstand seismic activity.

Table 7. The ratios of peak accelerations recorded at the 2^o floor and 1st floor of a building in Angra

| Events / Components. | E-W | N-S | Vertical |
|----------------------------------|------|------|----------|
| Main shock | 3.73 | 2.16 | 1.00 |
| Aftershock of July 11, at 00h49m | 4.71 | 3.46 | 1.84 |

As a final note of Section 3., we want to emphasize that since 1990, significant efforts have been made to equip the entire Azorean territory with seismological and accelerometric stations. This initiative aims to better understand (i) the seismic movements from the seismic source to various locations across the territory, (ii) the 'site effect' of certain formations, and (iii) the seismic behavior of different types of constructions.

4. Study of simple structures

To relate the observed movement or seismic behavior of certain simple structures with the seismic action at the foundation level or their support points, a selection of structures in Faial and Pico was made. Figure 12 presents the locations of these simple structures especially selected for analysis.

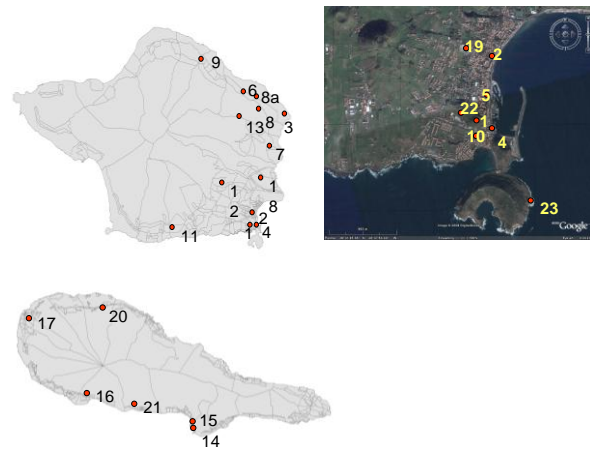


Figure 12. Places where it is possible to identify ground motion based on structural behavior of simple structures: 1 – Observatório Príncipe de Mónaco; 2 – Torre do Relógio; 3 – Farol da Ribeirinha; 4 – Estátua de Manuel Arriaga na Horta; 5 – Chaminé na Horta; 6 – Fonte Baptismal em Espalhafatos; 7 – Igreja de Pedro Miguel; 8 e 8^a – Centro da Ribeirinha; 9 – Casa Canada do Sousa; 10 – SRHE; 11 – Igreja da Feteira; 12 – Centro de Flamengos; 13 – Lomba grande; 14 – Quartel das Lajes do Pico; 15 – Chaminé nas Lajes do Pico; 16 – Ribeira do Cabo; 17 – Madalena; 18 – Cemitério Almojarife; 19 – Cemitério Horta; 20 – Cemitério Bandeiras; 21 – Cemitério São Caetano; 22 – Depósito Rádio Naval; 23 – Semáforos Monte da Guia.

These structures drew attention after the earthquake due to their movement or damage. The study was divided into two parts: the first part we applied analytical models to verify observations and quantify the incoming seismic action ("input"), while the second part we described behaviors, drawing only qualitative conclusions. In the future, it will be beneficial to select additional structures and apply analytical

models to expand the study's scope to more structures, such as the "março do Pico" (a ramble deposit in the shape of a pyramid that crumbled), windmills, landslides, etc. For the analytical studies conducted for the example in the following section, it was assumed that the seismic action at the foundation ("input") was based on the analog record from the Observatório Príncipe de Mónaco (Figure 4), with the amplitude scaled to match the observed behavior. Currently, efforts are focused on varying the seismic action based on the source generation (Zonno et al., 2008), adjusting it according to the location relative to the fault and the respective geotechnical conditions, to better reflect reality at each location.

4.1. Case Studies by numerical Modeling

Several case studies were developed using analytical models subjected to the Horta record (Figure 4) in an attempt to recover the seismic movement by leveraging the knowledge of the behavior of simple structures (Figure 12). These included: the Farol da Ribeirinha, a chimney, the statue of Manuel de Arriaga, the Torre do Relógio in Horta, and the Baptismal Font of the Church of Espalhafatos. For this purpose, mathematical models using Discrete Element Models (DEM) to attend to non-linear behavior and large displacements were developed (Oliveira et al., 2002), reproducing the mechanical characteristics of the structures under study. For the "Lomba Grande" Landslide we use the "Eulerian-Lagrangean Methods (Chen et al. 2025)².

The analysis of the analogue record obtained 15 km from the epicenter showed that the particle movement orbit in the horizontal plane, in terms of displacement, initially moves in the NNW-SSE direction, which aligns with observations made on different objects and structures, as previously described, i.e., approximately in the N-S direction. However, not all structures exhibit this movement. For example, the Torre do Relógio in the city of Horta, a landmark structure about 30 meters tall with a frequency of 1.4 Hz, experienced significant movement in the E-W direction, predominantly towards the West.

- The amplification observed at the Observatório Príncipe de Mónaco occurs at frequencies of 1.7 and 2.7 Hz, apparently decoupled from the fault mechanism, while the three major impulses in the N-S component or the two impulses in the E-W component are likely attributed to the fault rupture.

- The Farol da Ribeirinha (Figure 13) is a high-quality stone masonry structure, built in 1918 on top of a pyroclastic cliff. It is located about 5 km from the epicenter. The structure, including the tower and the keeper's house, suffered significant damage, with the tower rotating counterclockwise (viewed from above), and the section expanded due to the

stones opening at mid-height. There are signs of preferential movement in the NNE-SSW direction, both now and during the 1926 earthquake, which, although it did not cause damage, left an impact scar on the metal support of the optics.

- Analytically, the vibration frequency of the lighthouse is 4 Hz, dropping to 2.75 Hz when subjected to intense seismic action causing the observed type of damage. The measured in-situ frequency after the earthquake was 2.5 Hz, close to the analytical model. This study concluded that the seismic "input" action was 1.5 to 2 times the action recorded at the Observatório Príncipe de Mónaco, with a maximum acceleration of 0.6 to 0.8 g. - The Statue of Manuel Arriaga (Figure 14), located near the embarkation pier for Pico and about 500 m from the Observatory, showed a rotation of the statue relative to the pedestal of about 7° clockwise and a translation southward of 5 cm. Analytically, the input producing the response closest to reality suggests a seismic action about 70% of that recorded at the Observatory, i.e., 0.22g.

- Another case analyzed was a chimney in "Baixa" da Horta (Figure 15) about 1 km from the Observatory. Here, the result closest to reality points to 65%, or 0.20 g. - Closer to the epicenter (6 km), the case of the Baptismal Font of the Church (Figure 16) in Espalhafatos, which fell SSE, was analyzed. Although the calculation was heavily influenced by the parameter values assigned to the model, the best estimate points to a factor of 2 compared to the action at the Observatory, i.e., 0.6 to 0.8 g, similar to the estimates for the Farol da Ribeirinha.

- The Lomba Grande landslide (Figure 17) was analytically simulated using numerical modeling (Chen et al., 2025), and the observed reality aligns closely with the model results when a peak ground acceleration (PGA) of 0.60 g is adopted.

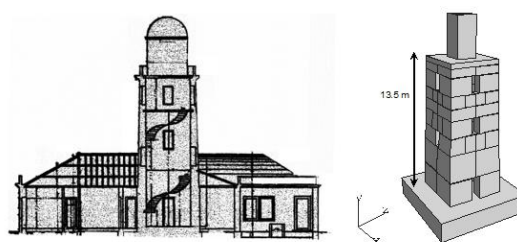


Figure 13. Vertical cross-section of Farol da Ribeirinha and developed analytical model ("discrete elements model", Oliveira et al., 2002).

² Malheiro et al. (1999) make an account of the various landslides, flush-soil, rock fall, etc. observed during the 1998 earthquake.

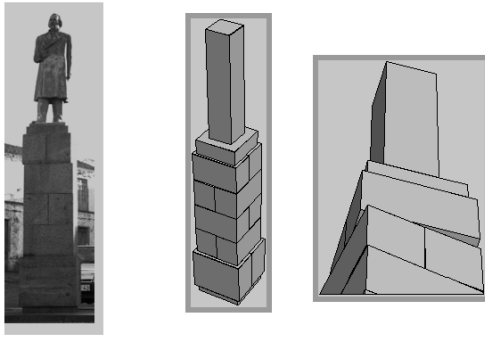


Figure 14. Statue of Manuel Arriaga in Horta (with upper part rotated) and developed model.

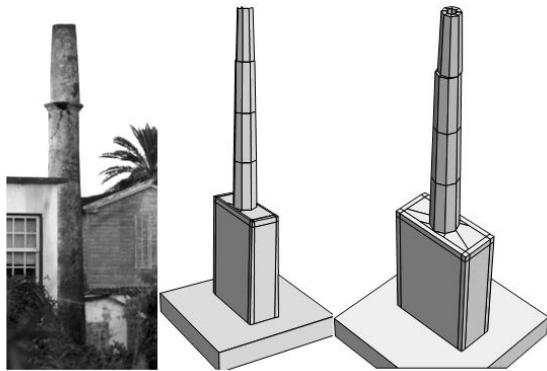
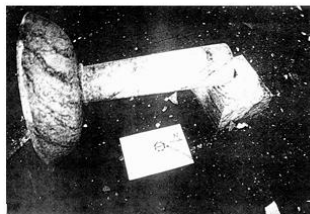
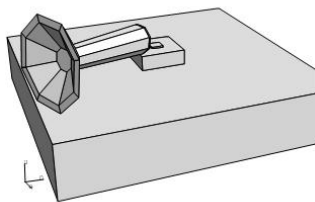


Figure 15. Old Chimney in Horta: a) damaged structure; b) developed model; c) deformed response.



a)



b)

Figure 16. Baptismal Font in Espalhafatos: a) collapse to the south; b) developed model.

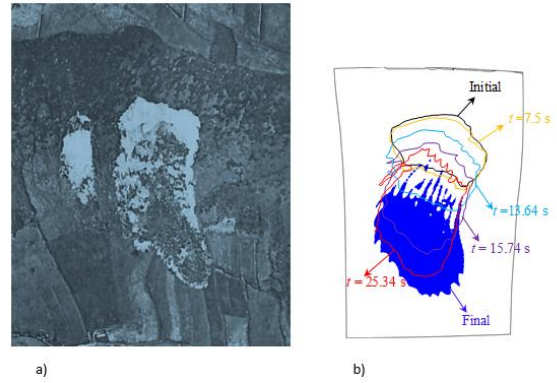


Figure 17. a) Plan view of the landslide in Lomba Grande; b) Modeling (Chen et al. 2025)

4.2. Other Cases

4.2.1. Faial

Other notable cases indicating the movement of settled bodies include several instances on Faial Island. On Faial Island, numerous cases reveal the preferential direction of soil movement. We will subsequently discuss the most interesting cases, commenting on the observed phenomena. Many gables of old stone masonry houses, constructed according to traditional methods, collapsed in a more or less widespread manner. Although a systematic study of the predominant direction was not conducted, it appears that the gables of houses in the parishes of Pedro Miguel, Ribeirinha, and Salão, which face south, more frequently collapsed in that direction (Figure 18).



Figure 18. Bulging and collapse of gable walls to the south.

In the case of the Casa da Canada do Sousa, in the transition from the parish of Salão to Cedros, already a bit further from the epicenter, a bulging to the south of the two gable walls was observed, without collapse, indicating a predominant push to the north. All these walls were poorly braced in the direction perpendicular to their plane, making them more vulnerable to 'out-of-plane actions.' Quick calculations based on out-of-plane wedge instability loads (by courtesy A. A. Costa, 2008) lead, for typical one-story houses with gables, to acceleration values around 0.3 g to cause gable collapse. In the houses of those same parishes with walls oriented in the N-S direction, the movement caused diagonal cracking in the plane, also indicating a predominant ground push to the north (Figure 19).



Figure 19. Cracking in walls in the N-S direction denoting the ground movement to the North (Freguesia da Ribeirinha).

In the city of Horta, there are several instances of bookshelves loaded with books falling over and leaning against the walls of houses. Let's examine two cases: one with a bookshelf collapse and another without issues. The first case occurred in the building annexed to the Prince of Monaco Observatory, which was notably shaken by the earthquake. Here, the bookshelf leaning against the south-facing wall fell, while the one against the north wall remained unaffected. The shelves against the east and west-facing walls also stayed intact, indicating a predominant ground movement to the north. In the main building, the paper earthquake recorders, placed along a north-south axis (with the ability to rotate east or west), remained upright, while another on an east-west axis swayed and fell to the north.

The second case involves the meeting room of the Regional Secretariat for Housing and Equipment (SRHE) building, located near the Observatory but in the lower part of the city. In this room, shelves leaning against the south, east, and west walls were unharmed, and in other rooms with different orientations, nothing unusual occurred. It is believed that the seismic activity in this area was much lower than at the Observatory.

In Feteira, the church tower showed movement in the north-south direction, resulting in a tilt to the south. In Flamengos, a region with soft soils, the seismic activity was more intense, causing significant destruction to many houses, the church, and the retaining wall near the Conceição water stream. In the cemetery, there are indications of stone movement in the north-south direction, and the widespread collapse of the retaining wall also occurred towards the south."

- The pinnacle of the south tower of the Church of Almoxarife fell to the south.

The Church of Ribeirinha, oriented nearly north-south, suffered major damage characterized by a global movement of the longitudinal walls with a tilt to the east and the collapse of the altar area to the south.

The Church of Pedro Miguel, oriented east-west, exhibited significant damage on the south side, indicating ground movement to the north and west. The bus stop shelter, constructed with cement blocks and located at Chão da Cruz on Regional Road No. 1 near the descent to Ribeirinha, shows

widespread cracking at the base, suggesting ground movement in the N45°E direction.

4.2.2. Pico

Other notable cases indicating the movement of settled bodies include several instances on Faial Island. On Faial Island, numerous cases reveal the preferential direction of soil movement. We will subsequently discuss the most interesting cases, commenting on the observed phenomena. Many gables of old stone masonry houses, constructed according to traditional methods, collapsed in a more or less widespread manner. Although a systematic study of the predominant direction was not conducted, it appears that the gables of houses in the parishes of Pedro Miguel, Ribeirinha, and Salão, which face south, more frequently collapsed in that direction (Figure 18). Unfortunately, on Pico Island, there are not as many notable cases as in Faial, possibly because the areas are further from the epicenter. The ground movement generally contrasts with what was observed on Faial, indicating movement in the south-southeast quadrant direction. The Lajes Fire Station is perhaps the most notable exception to this southward trend. It is a 1980s structure with a reinforced concrete frame and masonry block infill walls. The garage area features short columns due to the continuous windows at the top of the outer wall oriented north-south. As shown in Figure 20, the two columns of this wall have developed diagonal cracks, indicating ground movement to the north. The structure is located over 37 km from the epicenter, in a region where generally only minor damages were observed, but it exhibits an anomaly of significant localized damage in the Parish of Almagreira. Studies are underway to determine the level of seismic input capable of generating the forces that caused this cracking, both upper and lower thresholds. Initial calculations suggest a frequency of 2.0 Hz for the garage structure. The direction of movement may be linked to the polarization of that 2.0 Hz frequency in the north-south direction with a PGA of 0.2 g (Alves, 2009).



Figure 20. Fire HeadQuarter in Lajes-Pico: a) view of garage with shear cracks in columns; b) Damage in central column (outer view from West).

- The chimney at Lajes, located a short distance from the Fire Station, exhibited significant deformations at the top of the shaft, possibly due to higher modes, and signs of excessive compression near the base, indicating ground movement to the

north (Figure 21). It is noteworthy that Lajes do Pico is an area of positive anomaly in propagation with increased IMM intensity. The frequency of the chimney is estimated at 1.0 Hz by comparison with other chimneys of the same height (30 m).

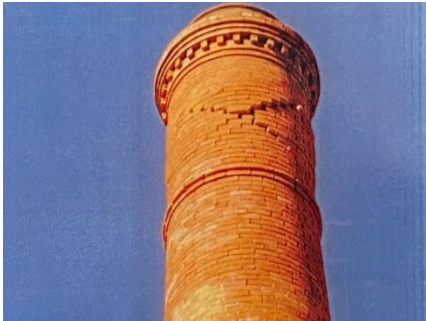


Figure 21. Damage to a tall brick chimney exhibiting cross fractures at the upper part.

Two stone masonry houses in the area of Ribeira do Cabo showed a very similar collapse of the gables to the west (Figure 22 a)). This phenomenon is also observed in Madalena (Figure 22 b)). The Church of São Mateus displayed a bulging of the north wall towards the north, suggesting ground movement to the south.



Figure 22Gables fallen to the West in Pico: a) Ribeira do Cabo; b) Madalena

The collapse of the gables to the west in Pico, as mentioned, indicates significant ground movement affecting these structures. Such damage can result from seismic activities that cause lateral displacements, leading to the collapse of the gables. Specifically, this occurred in stone masonry houses in Lugar de Ribeira do Cabo and Madalena. These observations are crucial for understanding structural behavior during seismic events and can assist in future studies on the resistance and vulnerability of constructions in the region.

4.3. Movement of standing objects

In many instances, standing objects were seen out of their initial positions, exhibiting translational movements, rotations, or mixed configurations. These cases are very common in cemeteries, either with heavy flower pots, labeling plates (Figure 23 a) and b)), or in columns or statues of individual carved stones on top of each other (Figure 24).

In cemeteries, flower boxes made of marble or other types of stone are commonly placed on the stone covering the graves. Movements of these objects were observed in various cemeteries on Faial and Pico (Figure 20), showing a consistent southward direction and a decrease in movement amplitude with increasing epicentral distance (Table IX). In the Horta Cemetery, a statuette (Figure 21) was also noted, with the pedestal rotating and shifting in a manner similar to the Statue of Manuel Arriaga, indicating seismic activity of approximately 0.20 g.

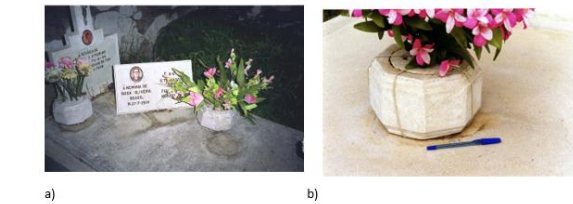


Figure 23 Movement of flower pots in cemeteries’: a) Ribeirinha; b) Horta.



Figure 24 Rotation movement in Horta cemetery: a) pedestal; b) detail of movement.

Table 8 summarizes the values of displacement observed in standing alone objects.

Table 8. Movement observed in flower pots in cemeteries

| Cemeteries | Epicentral Distance (km) | Displacement (cm) | Orientation of motion | Consistence in the observations |
|-------------|--------------------------|-------------------|-----------------------|---------------------------------|
| Ribeirinha | 5 | 17 | S10°W | Several cases |
| Almoxarife | 10 | 4-10 | S60°W | |
| Horta | 13 | 1-3 | S | w/rotation |
| Feteira | 16 | 1 | S | |
| Bandeiras | 20 | 3-6 | N/W | |
| São Caetano | 30 | 5-10 | W | w/rotation |

Another observation of the same type, near the Regional Road in Espalhafatos, involves the behavior of a set of 5 flower pots with narrow bases (Figure 25), which toppled to the East (N100°E), indicating ground movement to the West. Estimation of PGA to topple is of order 0.5 g.

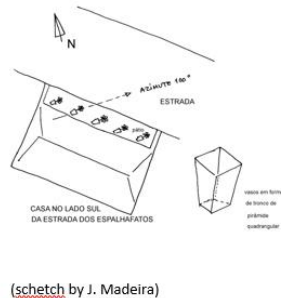


Figure 25 Movement of simple standing objects: all 5 flower pots fell to the East.

- As previously mentioned, in the City of Horta, seismic activity varied significantly not only in amplitude but also in frequency content. The Prince of Monaco Observatory is situated within part of a volcanic crater, forming a semi-cone of pyroclastic material with specific natural frequencies (see Oliveira et al., 2008). Nearby in the same crater, there is an abandoned elevated water tank belonging to the Naval Radio (Figure 26). This structure, with in-situ measured translation frequencies of 1.46 Hz and torsion frequencies of 2.22 Hz, did not sustain any damage. The same is true for the two structures (Semaforos-traffic lights for boats) on Monte da Guia, which, despite being very slender, also remained undamaged. For these latter structures, extrapolating from studies on the 1980 Earthquake in Terceira concerning similar structures (Oliveira et al., 1992)—where "empty - portal" presents a frequency of 1.69 Hz and "filled - with masonry" of 2.57 Hz—it can be concluded that the maximum acceleration there did not exceed 0.03 g.

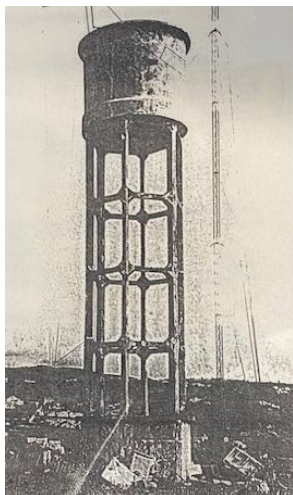


Figure 26 Elevated water tank exhibiting no damage to their structural elements

Estimated maximum acceleration values for various locations, where the structural behavior of simple structures was understood, are detailed in Table 9.

Table 9. PGA estimated for various locations in Faial Island, based on the interpretation of simple structures.

| Localization | Study Type | Epicentral Distance (km) | PGA (g) | Method used |
|---------------|---------------------------------|--------------------------|---------|-------------|
| Ribeirinha | Lighthouse | 5 | 0.6-0.8 | Model |
| Espalhafatos | Baptismal Font | 5 | 0.6 | model |
| Lomba Grande | Landslide | 7 | 0.6 | model |
| Salão-Cedros | Houses with collapsed gables | 8-10 | 0.4-0.3 | estimative |
| Horta | Observatory | 13 | 0.4 | measure |
| | Statue Manuel Arriaga | 13 | 0.22 | model |
| | Chinmey, Café Volga | 12 | 0.15 | model |
| | Clock Tower | 11 | 0.20 | model |
| | Statue, Cemetery | 12 | 0.20 | estimative |
| | Elevated Water tank Rádio Naval | 13 | <0.10 | estimative |
| Monte da Guia | Traffic lights for boats | 14 | 0.03 | model |
| Valverde | Marroços | 15 | 0.20 | estimative |
| Lajes | Tall Chimney (25 m) | 38 | 0.10 | estimative |
| Lajes | FireHouse | 39 | 0.15 | model |
| | | | | |

5. Attenuation of strong motion (PGA and Displacements) for the main shock

Figure 27 provides an assessment of the acceleration data reported in Table 9, just for the structures which were the object of analytical modeling, clearly showing how attenuation occurs with distance. These are the points of higher quality.

Based on the maximum values of the earthquake accelerations at the 05:19 earthquake, the attenuation of the main earthquake movement was estimated according to the law:

$$\ln a = c_1 + c_2 \ln(R) + c_3 R$$

where **a** is the maximum acceleration of the record; **R** is the distance from the station to the epicenter and the constants **c**₁, **c**₂ and **c**₃ are estimated by linear regression analysis from the peaks of the accelerometric recordings. Figure 27 illustrates the attenuation of maximum acceleration with the epicentral distance of the observed and predicted values. Attenuation reaches a "plateau" for epicentral distances less than 10 km.

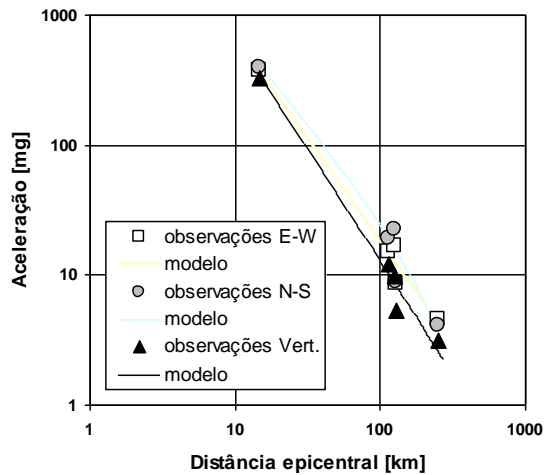


Figure 27 Attenuation of observed versus predicted values for the 5:19 earthquake. (white ellipse at top corresponds to the estimate of maximum acceleration at Farol da Ribeirinha – Figure 5- the closest inland point to the fault plane).

This visual marker aids in identifying discrepancies between actual recorded data and theoretical predictions. Significant deviations between observed and predicted values may suggest that local site effects or specific geological features are influencing seismic wave propagation. Such analyses are essential for refining predictive models and enhancing the accuracy of seismic hazard assessments. Table 10 compiles the constants of the attenuation models plotted in Figure 27, along with the root mean square errors (RMSE) of the estimates for each component. The abbreviation "ns" indicates that, according to the t-test, the constant is not significantly different from zero. In such cases, the regression was redone, excluding the non-significant variable. Notably, when extrapolating the model's application to very short distances (5 km), the results generally align with studies conducted for the Farol da Ribeirinha (Sincrain et al., 1999). This suggests that the model's predictions remain robust even at shorter distances, supporting its validity and usefulness in seismic hazard analysis for that region.

Table 10. Values of constants in the attenuation law.

| Const. / Comp. | E-W | N-S | Vertical |
|----------------|---------|---------|----------|
| c1 | 1.4360 | 1.1299 | 1.4912 |
| c2 | -1.5816 | -1.2692 | -1.67321 |
| c3 | ns | -0.0020 | -0.0003 |
| RMSE [mg] | 1.06 | 1.85 | 0.73 |

If we include all other points beyond those of high quality, we find the plot of Figure 28, where we separate the values for acceleration from the values for displacement (Tables 8 and 9).

The attenuation laws for maximum acceleration with distance, estimated in this study specifically for magnitude 6.0 earthquakes, are currently undergoing more comprehensive

analysis. These studies aim to incorporate magnitude as an independent variable in the model. In addition to aftershocks from the 1998 crisis, they are using data from other seismic events, such as the 1997 crisis and the earthquakes of 1980 and 1973, along with all the information collected from the new accelerometric network in the Azores. This expanded dataset will enhance the model's accuracy and reliability, providing a more nuanced understanding of seismic behavior in the region and improving predictive capabilities for future events.

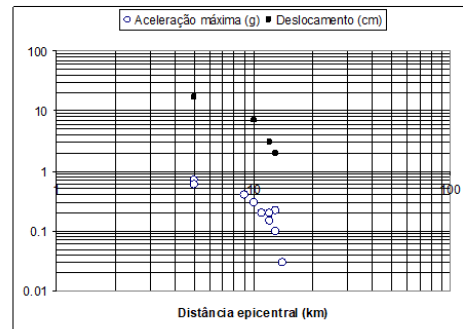


Figure 28 Attenuation of accelerations and displacements of supported structures with epicentral distance (data: local observations – Tables 8 and 9).

Finally, in Figure 29 we compare various acceleration (PGA values) of larger Azores earthquakes on which we have some type of information with values captured in a few stations for events felt in Iceland with a similar volcanic environment compared to Azores.

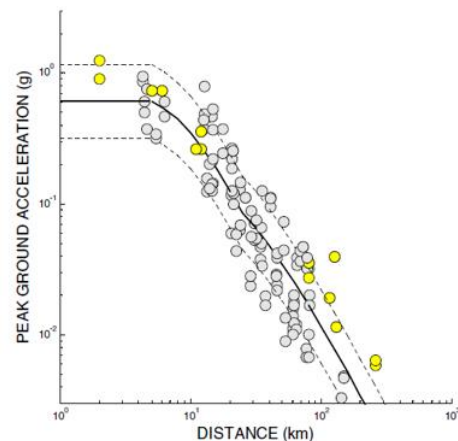


Figure 29. Comparison among ground motion recorded in Azores and Iceland events. Recovered from Oliveira et al. (2004): PGA in Azores (yellow dots) and in Iceland (gray dots). Earthquake included are: 23 November 1973, 01:36 (Azores); 1 January 1980, 16:43 (Azores); 9 July 1998, 05:19 (Azores); 17 June 2000, 15:41 (South Iceland); 17 June 2000, 15:43 (South Iceland); and 21 June 2000, 00:52 (South Iceland). The data applied have been extracted from the ISED Website and scaled to magnitude 6.6

6. Discussion

This work aims to present the records of seismic movement in various locations and attempts to relate them to the observed behavior in some structures. Propagation studies, now presented, should in the future include data from other earthquakes and the so-called 'site effect.' It also aims to deepen the understanding of how the rupture occurred in the fault that generated the earthquake. In summary, it can be said that the evidence of ground movement to the North in Faial and to the South and West in Pico suggests a rupture in a NNW-SSE, left-lateral fault (Figure 3), which begins at a point to the North and propagates South until a rapid stop asperity to cause such movement. This preliminary interpretation complements that of Borges et al. (2007) with the proposal of the existence of two main nuclei in the fault rupture. This first movement, of high frequency ($f > 5$ Hz), which affects small constructions, is followed by lower frequency waves ($1 < f < 3$ Hz) with large amplitude and E-W polarization, which affects larger or taller constructions. Further clarification of these matters involves, on one hand, a thorough study of all existing elements from various areas of geophysical sciences and seismic engineering, from which more information has now been gathered and can be used to complement the existing observations especially in places where there are no Strong Motion Records.

The type of work presented here can be applied to more recent events, utilizing additional information captured from video camera footage, which provides insights not only into the final result of the shaking but also into the mechanisms during the shaking.

Acknowledgements:

Carlos Sousa Oliveira is grateful for the Portuguese Foundation for Science and Technology's support through partial funding UIDB/04625/2025 from the research unit CERIS.

References

- Alves, J.P. (2009). Estudo Sísmico do Quartel de Bombeiros das Lajes, Pico. MSc thesis, IST, Lisbon.
- Ambraseys N.N. et al. 2002 "ISESD (<http://www.isesd.cv.ic.ac.uk>) – Internet Site for European Strong-Motion Data." European Commission, Research-Directorate General, Environment and Climate Programme.
- Borges, J.F.; Bezzeghoud, M.; Buforn, E.; Pro, C.; Fitas, A. (2007). The 1980, 1997 and 1998 Azores earthquakes and its seismotectonic implications. *Tectonophysics*, 435, 37-54.
- Caldeira, B.; Fontiela, J.; Borges, J. F.; Bezzeghoud, M. (2017). Grandes terremotos en Azores. *Física de la Tierra*, 29, 29-45.
- Carrilho, F.; Custódio, S.; Bezzeghoud, M.; Oliveira, C. S.; Marreiros, C.; Vales, D.; Alves, P.; Pena, A.; Madureira, G.; Escuer, M.; Silveira, G.; Corela, C.; Matias, L.; Silva, M.; Veludo, I.; Dias, N.; Loureiro, A. A.; Borges, J. F.; Caldeira, B.; Wachilala, P.; Fontiela J. (2021). The Portuguese National Seismic Network —Products and Services, *Seismol. Res. Lett.* XX, 1–30, doi: 10.1785/022020040711.
- Chen, X., Fernández F., Vargas E., Oliveira, C.S., Inácio, M., Sousa, L.R., Malheiro, A., Sousa, R.L. (2025). 3D large-deformation modeling of Lomba Grande landslide runout using coupled Eulerian-Lagrangian method. Paper submitted to ISRM Workshop on Soft Rocks, FEUP, Porto.
- Dessai et al. (1999). The record of July 9 1998 Earthquake at the Chã de Macela Downhole IRIS Station. *Proceedings 4th Meeting on Seismology and Earthquake Engineering*. EST/ Universidade do Algarve, Faro. (in Portuguese).
- Dias, N.A.; Matias, L. (2008). Specific studies with seismic networks for detailed seismic characterization. In *Sismo 1998. Açores, Uma década depois*. Ed C.S. Oliveira, A. Costa, J.C. Nunes, SPRHI SA, 89-98 (in Portuguese).
- Fontiela, J.; Oliveira, C.S.; Rosset, P. (2018). Characterisation of Seismicity of the Azores Archipelago: An Overview of Historical Events and a Detailed Analysis for the Period 2000–2012. In U. Kueppers and C. Beier (eds.), *Volcanoes of the Azores, Active Volcanoes of the World*, pp 127-153. https://doi.org/10.1007/978-3-642-32226-6_8.
- Fructuoso, G. (1873). *Saúdaes da Terra*, Vol 1-6. Ponta Delgada (Azores), Portugal: Instituto Cultural de Ponta Delgada, ISBN 972-9216-70-3.
- Lopes, I.; Deidda, G.P.; Mendes, M.; Strobbia, C.; Santos, J. (2013). Contribution of in situ geophysical methods for the definition of the São Sebastião crater model (Azores). *Journal of Applied Geophysics*, 98, 265-279.
- Malheiro, A.; Fraga, C.; Oliveira, C.S. (1999). Escorregamentos e Danos nas Vias de Comunicação Causados pelo Sismo de 9 de Julho de 1998 no Faial-Pico-São Jorge, *Proceedings 4th Meeting on Seismology and Earthquake Engineering*, EST/Universidade do Algarve, Faro (in Portuguese).
- NP EN 1998-1 (2010). Eurocódigo 8 – Projecto de estruturas para resistência aos sismos – Parte 1: Regras gerais, ações sísmicas e regras para edifícios (in Portuguese).
- Nunes, J.C.; Forjaz, V.H.; Oliveira, C.S. (2004). Seismic catalog of the Azores region. Version 1.0 (1850-1998). *Proceedings 6th Portuguese Congress of Seismology and Seismic Engineering*, Ponta Delgada, 349-357.
- Oliveira, C.S.; Costa, A.C.; Forjaz, V.H.; Nunes, J.C. (1990). Seismic hazard analysis in zones of time and space interdependence: An application to São Miguel Island, Azores. *Natural Hazards*, 3(1), 15–29.
- Oliveira, C.S. (1992). Quantificação do movimento sísmico aquando do sismo de 1 de Janeiro de 1980. In *Monografia 10 Anos após o sismo dos Açores de 1 de Janeiro de 1980. Aspectos Técnico-Científicos*, Ed. CS Oliveira, ARA Lucas e JH Correia Guedes. Vol. 1, 83-126, SRHOP/LNEC. (in Portuguese).
- Oliveira, C.S.; Lemos, J.V.; Sincrain, G.E. (2002) Modelling Large Displacement of Structures Damaged by Earthquake Motions. *European Earthquake Engineering*, Vol 3, 256-76.

- Oliveira, C.S., Sigbjornsson, R., Olafsson, S. (2004). A comparative study on strong ground motion in two volcanic environments: Azores and Iceland. *Proceedings 13th World Conference on Earthquake Engineering*, Vancouver BC, Canada, paper no. 2369.
- Oliveira, C.S. (2008). Os registos do movimento sísmico obtidos na rede acelerográfica dos Açores. Comparação com outros indicadores do movimento sísmico. In *Sismo1998. Açores, Uma década depois*. Ed C.S. Oliveira, A. Costa, J.C. Nunes, SPRHI SA, 119-136. (in Portuguese).
- Oliveira, C.S.; Nunes, J.C.; Ferreira, M.A. (2008). Apontamentos sobre a avaliação de perigos geológicos nas Ilhas do Faial e Pico na sequência do sismo de 9 de Julho de 1998. In *Sismo 1998. Açores, Uma década depois*. Ed C.S. Oliveira, A. Costa, J.C. Nunes, SPRHI SA, 379-384 (in Portuguese).
- Oliveira, C. S. (2025). Personal Communication, In preparation.
- RSA (1983). Regulamento de Segurança e Acções para Estruturas de Edifícios e Pontes. Imprensa Nacional, Lisboa. (in portuguese). Seismosoft (2021) <https://seismosoft.com/products/seismosignal/>.
- Senos, M.L. (2008). The July 9, 1998 Azores Earthquake and the aftershock sequence-revisited 10 years later. In *Sismo 1998. Açores, Uma década depois*. Ed C.S. Oliveira, A. Costa, J.C. Nunes, SPRHI SA, 74-87 (in Portuguese).
- Sincraian, M.V.; Oliveira, C.S. (1998). Non-Linear Seismic response of a Volcanic Hill using the Finite Element Method. *Proceedings 9th International Conference of Soil Dynamics and Earthquake Engineering*. Bergen, Norway.
- Stucchi, M.; Rovida, A.; Gomez Capera, A.A.; Alexandre, P.; Camelbeeck, T.; Demircioglu, M.B.; Gasperini, P.; Kouskouna, V.; Musson, R.M.W.; Radulian, M.; Sesetyan, K.; Vilanova, S.; Baumont, D.; Bungum, H.; Fäh, D.; Lenhardt, W.; Makropoulos, K.; Martinez Solares, J.M.; Scotti, O.; Giardini, D. (2013) The SHARE European earthquake catalogue (SHEEC) 1000–1899. *J Seismol* 17(2):523–544. <https://doi.org/10.1007/s10950-012-9335-2>.
- Vilanova SP, Ferreira MA, Oliveira CS (2009) PAD-1.0 Portuguese accelerometer database, CD-ROM edition. *Seismol Res Lett* 80(5):839–844.
- Zonno, G. (2008). Keynote Lecture. In *Proceedings Int. Seminar on Seismic Risk and Rehabilitation, on the 10th Anniversary of the July 9, 1998 Azores Earthquake*. Ed. CS Oliveira et al. SPRHISA